

FEASIBILITY STUDY OF A NOVEL, FAST READ-OUT SYSTEM FOR AN IONIZATION PROFILE MONITOR BASED ON A HYBRID PIXEL DETECTOR

O. Keller, B. Dehning, S. Levasseur, M. Sapinski, CERN, Geneva, Switzerland

Abstract

The ability to continuously monitor the transverse beam size is one of the priorities for the upgrade and consolidation of the CERN Proton Synchrotron for the High Luminosity LHC era. As well as providing an average beam size measurement throughout the acceleration cycle, the requirements also cover bunch-by-bunch measurements of up to 72 bunches with a spacing of 25 ns within 1 ms. An ionization profile monitor with a hybrid pixel detector read-out is therefore being investigated as a possible candidate to provide such measurements. In this contribution the concept, based on a Timepix chip, is presented along with first laboratory measurements showing the imaging of low-energy electrons in vacuum.

INTRODUCTION

Ionization Profile Monitors (IPM) are devices measuring the transverse size of a particle beam. Electrons or ions resulting from ionization of the residual gas in the beam vacuum are extracted and used to reconstruct the beam profile. Electrons are used if fast measurements are required. They are accelerated towards a detector by an electric field. In addition a parallel magnetic field provides confinement of their orbits along the electric field lines.

Two main types of electron readout systems are commonly used in the current IPMs:

- Multi-strip metal anodes, e.g. at Fermilab [1], BNL [2] and J-PARC [3].
- Optical readout, based on the conversion of electrons into light which is captured by a camera, e.g. in the LHC [4, 5] or at GSI [6].

Both of these methods require amplification of the electron signal in front of the detector which is achieved by Multi-Channel Plates (MCP). Here a novel system based on the emerging technology of hybrid pixel detector is investigated. The detector consist of two pixelated elements, a sensor slab and a readout chip. The sensor reassembles an array of diodes operating in reverse-bias mode. A charged particle traversing the sensor generates free charge carriers in the material which are converted into a voltage pulse and further analyzed by the readout chip.

The Timepix3 is currently the most versatile and one of the fastest hybrid pixel detector readout chips available. It was developed within the Medipix Collaboration hosted by CERN and the first chips have been tested in 2013 [7]. It is designed for a sensor size of $14 \times 14 \text{ mm}^2$ and a resolution of 255 by 255 pixels. The size of one pixel is $55 \times 55 \mu\text{m}^2$.

When bump-bonded to a thin silicon sensor, the hybrid detector becomes sensitive to single low-energy electrons of a few keV. With the ability to set a threshold per pixel, high and homogeneous signal-to-noise ratios can be maintained. The pixels can operate in one of three measurements modes: deposited charge (TOT mode), time of arrival (TOA) and counting the number of events together with the total charge in one shutter period (PC/iTOT). The digital link transceivers of Timepix3 can send the recorded data continuously at a maximum hit rate of 85 Mhits/s/chip or $42.5 \text{ Mhits/s/cm}^2$.

The main advantages of the proposed technology are:

- The thickness is reduced with respect to the optical readout method, since no bulky light guides are needed; a magnet with a smaller aperture can be used.
- The fast readout speed enables to measure the beam size bunch-by-bunch with a spacing of 25 ns.
- No need for MCP amplification; MCPs exhibit complex behaviour in cases of prolonged usage with strong and highly repetitive input signals [8].
- Coupling to beam RF fields is expected to be small.
- Currently available charge integrators for strip detectors, with a comparable fast readout like the QIE10 [9], are orders of magnitude less radiation hard than the readout chips of the Medipix/Timepix family [10].

In addition to the readout system, we investigate here the geometry of the electrodes providing the extraction field.

OPERATIONAL SPECIFICATION

The circumference of the CERN Proton Synchrotron [11] is 628.3 meters and the revolution time varies from $\tau_{\text{rev}} = 5.63 \mu\text{s}$ for Pb^{54+} beams at injection to $2.1 \mu\text{s}$ for proton beams. It was first put in operation in 1959. Today it is used to generate a broad variety of beams: for test beam areas, fixed target experiments and for the LHC [12]. The proton beams in PS undergo transition crossing and bunch splitting - two phenomena which severely affect the beam emittance.

Operators of any accelerator would like to measure the beam parameters in the best possible way, however the technology does not always allow to fulfill their requests. In case of transverse profile measurements the operational specification for the foreseen PS upgrade is as follows:

1. Continuous, bunch-by-bunch monitoring of the beam emittance over the machine acceleration cycle (2.1 s) with an acquisition rate of 0.1-1 kHz.

2. Turn-by-turn measurement of a single bunch emittance.
3. Main use: qualification of LHC beams. These beams are small, therefore 5 cm of detector width will be enough to perform the measurements (vacuum chamber horizontal dimension is 15 cm).

Currently installed emittance monitors - wire scanners - cannot fulfill these specification. They can perform measurements only every several seconds and the two planes are multiplexed. In addition with the increase of the beam brightness planned by the LHC Injection Upgrade (LIU) project [13], scanners may suffer from extensive carbon fibre sublimation [14], which may restrict their use for certain beams.

The beam amplitude function varies between $\beta_{x,y} = 12-22$ m and dispersion $D_x = 2.4-3.2$ m. In the following calculations $\beta_x = 12$ m and $D_x = 2.4$ m are assumed as these are the values in the probable future location of the IPM.

ELECTRON RATES

The static pressure in the PS machines reaches $p = 10^{-9}$ mbar during operation since no bake-out is performed in advance. The composition of the rest gas is initially dominated by water and CO₂. The ionization cross sections for various gases calculated according to Bethe model (cf. [15]) are shown in Table 1. A conservative assumption that the residual gas is mainly composed of hydrogen (H₂) is used in the following calculations, but one should keep in mind that about 5-10 times higher rates can be expected.

Table 1: Ionization Cross Section for Different Gases and Beams

| | $\sigma_{ion,p}$ 2 GeV [Mbarn] | $\sigma_{ion,p}$ 25 GeV [Mbarn] | $\sigma_{ion,Pb54+}$ 15 GeV [Gbarn] | $\sigma_{ion,Pb54+}$ 1.2 TeV [Gbarn] |
|------------------|--------------------------------------|---------------------------------------|---|--|
| H ₂ | 0.19 | 0.23 | 2.6 | 0.6 |
| H ₂ O | 0.76 | 0.95 | 11 | 2.3 |
| CO ₂ | 1.32 | 1.66 | 19 | 4.0 |
| Ne | 0.43 | 0.55 | 6.0 | 1.3 |
| Ar | 0.9 | 1.16 | 12 | 3.0 |
| Xe | 1.7 | 2.2 | 24 | 5.3 |

The number of electrons produced per bunch and per machine turn is estimated from:

$$n_e = d \cdot \sigma_{ion} \cdot N_b \cdot p \cdot \frac{N_A}{R \cdot T} \quad (1)$$

where N_b is number of particles per bunch, N_A the Avogadro constant, R the ideal gas constant and $T \approx 293$ K.

Table 2 shows the typical number of electrons (n_e) expected to be produced by a single bunch, assuming that they are collected along an active detector length of $d = 15$ mm. The low number of electrons emitted per bunch show that turn-by-turn measurements will be difficult to achieve since

the relative error on the gaussian width is roughly equal to $1/\sqrt{n_e}$ (cf. figure 3.32 in [16]). Consequently a minimum acquisition of 10^4 electrons is needed to limit the error to 1% for the beam profile reconstruction. In order to increase the number of electrons per bunch, an injection of a heavy noble gas may be foreseen. An increase of the pressure together with the cross section could lead to a 1000-fold increase of the signal. However, the pressure bump would have to be confined around the IPM because of its influence on the emittance of ion beams. Another method would be to increase the pixel detector length. The good field region is designed to be 50 mm long, thus an installation of four Timepix detectors along the beam would allow to increase the signal.

Table 2 shows also the expected hit rates which approach the limits of state-of-the-art pixel detector readout chip capabilities:

- R_{chip}^{av} is the averaged hit rate per chip over a machine revolution period.
- R_{chip}^{max} is the hit rate per chip within a bunch.
- R_{pixel}^{av} is the average rate at which pixels below the beam center are triggered per machine revolution period.

READOUT MODES

The Timepix3 readout chip consist of an analog front-end and digital back-end to distribute the recorded hit data. Both parts impose their own constraints on the readout possibilities in the proposed IPM. The predecessor chip, Medipix3, showed a continuous front-end readout capability of about 2 MHz/pixel [17]. Since the Timepix3 front-end is designed for faster pulse processing, an even better performance is expected. If the maximum pixel hit rate would be surpassed, the pulse processing signal of these pixels in the front-end would be constantly over threshold rendering the data output unusable. In order to limit this rate on the detector front-end, the usage of a gating grid controlled by a fast HV switch in front of the sensor is considered. An accurate trigger signal is critical in this case.

The second constraint stems from the digital back-end. The Timepix3 uses eight low voltage differential data lines (SLVS type) plus one clock line to distribute the recorded hit data. In the nominal maximum speed configuration these lines can transmit at a rate of 640 Mbit/s resulting in 5.12 Gbit/s (including 8b/10b line encoding) of data per Timepix3 chip. Divided by 65k pixels and a gross data packet size of 60 bits per pixel, this results in the mentioned maximum hit rate of 85 Mhits/s/chip. Multiplied by a bunch spacing of 25 ns we can recover about two electron hits per bunch, if every pixel is operated in the TOT+TOA or TOA only mode. While the evaluation of the TOT value may be interesting to compensate for the charge sharing effect in silicon pixel sensors, the TOA only mode bears the advantage of an additional pile-up counter. This counter enables the conservation of otherwise missed hits occurring between consecutive data transmissions.

Table 2: Electron Production Rate for Various Beams

| name particles | achieved 25 ns | | LIU 50 ns | | HL-LHC 25 ns | | LHC ion | |
|---|----------------|------|-----------|-----|--------------|------|-------------------|-------------------|
| | p | p | p | p | p | p | Pb ⁵⁴⁺ | Pb ⁵⁴⁺ |
| E _k [GeV] | 1.4 | 25 | 2 | 25 | 2 | 25 | 15.02 | 1227 |
| emittance [μm] | 2.25 | 2.36 | 1.7 | 1.8 | 1.8 | 1.9 | 0.7 | 1.0 |
| N _b [$\cdot 10^{10}$] | 168 | 13 | 189 | 30 | 325 | 25.7 | 0.03 | 0.025 |
| bunch length ($4\sigma_1$) [ns] | 180 | 3 | 205 | 3 | 205 | 3 | 200 | 4 |
| $\Delta p/p$ [10^{-3}] | 0.9 | 1.5 | 1.0 | 1.5 | 1.5 | 1.5 | 1.2 | 1.1 |
| σ_{beam} [mm] | 3.9 | 3.7 | 3.5 | 3.7 | 4.4 | 3.7 | 4.0 | 2.9 |
| number of bunches (n _b) | 6 | 72 | 6 | 36 | 6 | 72 | 2 | 2 |
| n _e (H ₂) | 13 | 1 | 14 | 2 | 24 | 2 | 30 | 5 |
| R _{chip} ^{av} [MHz] = $\frac{n_e \cdot n_b}{\tau_{rev}[s]}$ | 37 | 34 | 40 | 34 | 69 | 69 | 11 | 4.8 |
| R _{chip} ^{max} [GHz] = $\frac{0.68 \cdot n_e}{2 \cdot \sigma_1[s]}$ | 0.1 | 0.5 | 0.1 | 0.9 | 0.2 | 0.9 | 0.2 | 1.7 |
| R _{pixel} ^{av} [kHz] = $\frac{n_e \cdot n_b \cdot 55[\mu\text{m}]}{255 \cdot \sigma_{beam}[\mu\text{m}] \cdot \tau_{rev}[s]}$ | 2.0 | 2.0 | 2.5 | 2.0 | 3.4 | 4.0 | 0.2 | 1.7 |

Besides different measurement modes per pixel, Timepix3 can be operated in two acquisition modes: event-based or frame-based. In frame-based mode an external shutter signal sets the exposure time for the whole frame. This acquisition mode is mandatory for the accumulative iTOT pixel mode. However, using the external shutter signal can be also useful in combination with the TOT and TOA pixel modes. It provides means to throttle the data output for certain bunch schemes where n_e is higher than required to recover the beam size. The iTOT mode is the only possibility for recording the whole profile of a single bunch at once. Consecutive measurements will be delayed based on the number of recorded hits. For continuous bunch-by-bunch measurements over multiple machine cycles the event-based mode is better suited. It has the advantage that no bunch-synchronous external trigger signal is required to control the shutter. Because of changes in the cycle period, complex bunch splitting and merging processes (often referred as RF gymnastics) it is necessary to use special techniques to detect bunch presence and position. A possible mechanism is presented in [18].

RADIATION LEVELS

During every machine cycle a small part of the beam is lost due to various mechanisms, originating from beam-gas interaction, beam instabilities and particles hitting the aperture limits. These losses have been simulated for a standard PS cell. Results are visualized in Fig. 1. In the center of the cell, close to the beam, the yearly dose reaches 10 kGy. The sensor and the Timepix3 detector shall withstand at least this dose in order to be not exchanged more often than once per year. Additional radiation monitors have been installed in the planned device location in order to compare the measurements with simulations.

When operated at maximum speed, the digital SLVS links of Timepix3 need to be handled by an FPGA. Currently, there is no fast enough and radiation hard transceiver like the GBTx available that could convert the signals into long-distance optical fiber links. In first chip tests, 3 m of SCSI ca-

bles with VHDCI connectors have been successfully used to connect the Timepix3 data lines to the FPGA-based SPIDR readout board developed by NIKHEF.

With few meters of cable, the FPGA could be installed under a shielding visible under the beam line in Fig. 1 or away from the beam pipe in the PS utility funnel, which reduces the dose by about a factor 10. The radiation hardness of Timepix3 is expected to be larger than the one of the sensor. In order to extend the lifetime of the sensor by limiting the radiation damage effects, it is planned to cool it down to about 0°C.

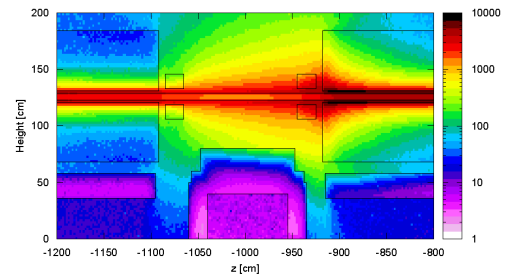


Figure 1: Radiation field in the typical PS straight section. The radiation is produced by beam-gas interaction. A shielding is proposed under the beam pipe in order to protect radiation-sensitive tunnel electronics. The radiation level is expressed in Gy/year. Courtesy of J.P. Saraiva.

ELECTRIC CAGE

The electric cage is a set of electrodes designed to provide a uniform electric field along the electrons path. The magnitude of the electric field has negligible impact on the profile deformation [19], but it must extract and accelerate electrons to energy levels which allow an efficient detection. With thin silicon sensors the efficiency reaches 100% for electrons of about 10 keV energy, therefore it is proposed to operate at an extraction voltage of at least 20 kV. The electric cage is also the main support structure of the device. Studying existing IPMs revealed a large variety of approaches to the

cage design. Several of these designs were investigated as possible candidate for the new IPM.

In order to be compared, all cages were modeled and simulated using the software suite CST Studio. Each design was adapted to our dimension requirements and only the field shaping elements were taken into account (top, bottom and side electrodes). Some designs were also modified in order to extend our comparison panel. Such designs include the cage from BNL and the cage from the LHC-BGI [4]. Figure 2 shows one of the modeled cages.

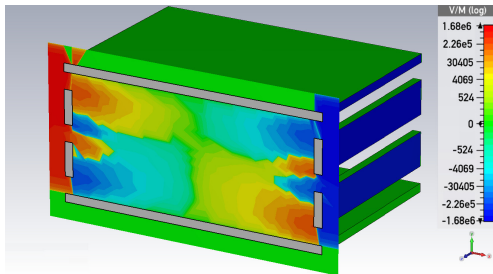


Figure 2: Plot of the electric field in the cross-section of the modified LHC-BGI design.

The electrostatic simulations give a complete picture of the electric field in each cage, while the particle tracking simulations are used to map the behavior of electrons along the transverse and vertical paths. The initial energy of the electrons is 5 eV [20]. Moreover, the effects of a 0.2 T magnetic field are also taken into account.

After post-processing an estimation of the electron signal distortion caused by the non-uniformity of the electric field was obtained. This estimation was used to compare the different cages and choose the best suited for our requirements. In total eight cages were studied and six proved to be relevant. As can be seen in Fig. 3, the comparison of the relative broadening of the beam size shows a clear leading of the modified LHC-BGI design.

In addition, it was found that the magnetic field of 0.2 T improves the signal distortion due to electric field nonhomogeneity by up to three orders of magnitude. Such a field is also needed to overcome the space-charge driven profile distortion as described in [20]. A special magnet is being designed for the future PS IPM. Because of the impact on the beam trajectory, the magnet will contain a region with inverted magnetic field compensating for the effect within the IPM itself. Detailed results of the electric cage study will be published later.

TESTS WITH LOW-ENERGY ELECTRONS

In order to prove the concept of measuring low-energy electrons with the proposed detector a test setup has been constructed. The electric cage used in these tests is an old cage from a IPM of the SPS machine. It is equipped with

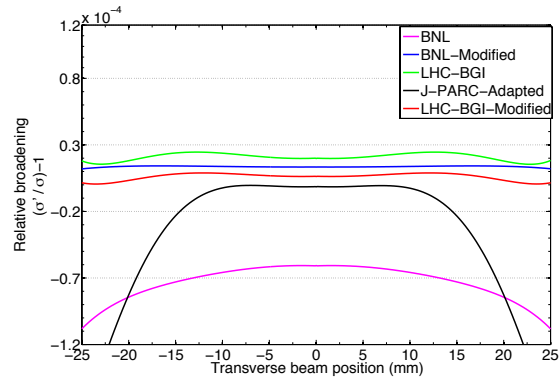


Figure 3: Relative broadening of the reconstructed beam size as a function of the transverse beam position.

an Electron Generation Plate (EGP) which is a cold and uniform electron source.

A Fitpix USB adapter housing a Timepix1 chip bonded to a 100 μm silicon sensor is placed at a distance of 10 cm from the EGP. The sensor is of p-on-n type. Instead of the common surface metallization, a thin n+ doped layer is used to provide the sensor bias voltage of 20 V. This leaves the detector sensitive to light, requiring a shaded operation, but also enables the penetration of low-energy electrons into the depletion region.

The detector is powered and connected to a computer via USB by a vacuum feedthrough. The electron hits are recorded with the Pixelman software and analyzed in the ROOT-based MAFalda framework [21].

The signals have been observed for extraction voltages of 3 to 5 kV. The system was running for several days and no degradation of the signal has been observed. As a byproduct of the experiments a clustered emission from the EGP was observed. This effect was unknown before because a much longer integration time is used in the previous optical readout method. Thanks to the short shutter times of the Timepix1, it can be seen that cascades of electrons are emitted from small areas of the EGP. However, after adding up many of these cascades, the distribution of the electrons is uniform as the EGP specification states. The background and signal images are shown in Fig. 4 for an extraction potential of 4.5 kV, Timepix shutter period of 10 ms and a pressure of about $6 \cdot 10^{-6}$ mbar. Because of the clustered emission it is not possible to obtain the energy spectrum of single electrons in this setup.

CONCLUSIONS

This preliminary study shows that a continuous beam emittance monitoring can be achieved in the CERN Proton Synchrotron by an Ionization Profile Monitor equipped with hybrid silicon pixel detectors based on Timepix3. This modern technology allows to perform fast, bunch-by-bunch measurements of the beam emittance during the PS acceler-

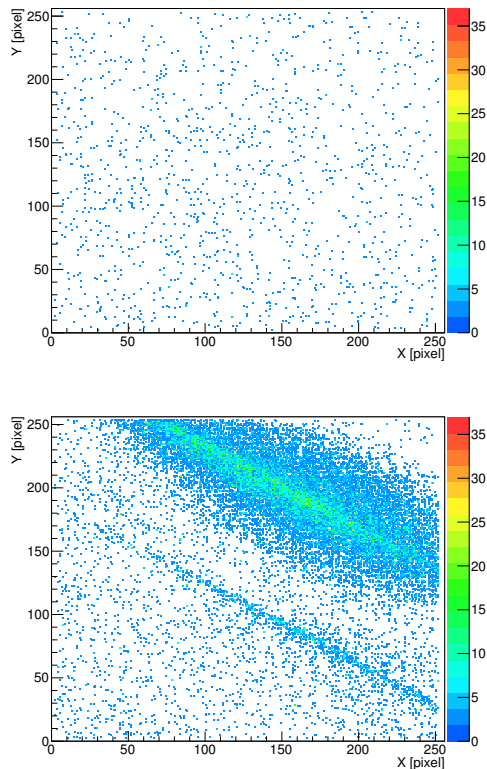


Figure 4: The image above shows the background. Below are electron clusters emitted from the EGP. An extraction potential of 4.5 kV was applied in both cases. The strong non-uniformity of the electric field close to the detector in the test cage is supposedly producing the stripe shape.

ation cycle. It is expected that the chip-sensor assembly will withstand radiation damage for at least a period of 2-3 years.

ACKNOWLEDGMENT

The authors want to thank numerous people from CERN and NIKHEF, especially: Xavi Llopart, Michael Campbell, John Idarraga, Simone Gilardoni, Django Manglunki, Heiko Damerau, Joao Saraiva, Jose Ferreira, Dominik Vilsmeier, Dominique Bodart, Didier Steyaert, Romain Ricol, Gerhard Schneider, Aniko Rakai, Jan Visser and Piotr Pacholek.

REFERENCES

- [1] J. Zagel et al., "Operational use of Ionization Profile Monitors at Fermilab", BIW'10, Santa Fe, 2010, TUPSM009.
- [2] R. Connolly et al., "Residual-Gas-Ionization Beam Profile Monitors in RHIC", BIW'10, Santa Fe, 2010, TUPSM010.
- [3] H. Harada et al., "Upgrade of Ionization Profile Monitor in the J-PARC 3-GeV RCS", IPAC'12, New Orleans, 2012, MOPPR029.
- [4] CERN IPM website: <http://cern.ch/bgi>

- [5] M. Sapinski et al., *The First Experience with LHC Beam Gas Ionization Monitor*, IBIC'12, Tsukuba, 2012, TUPB61.
- [6] T. Giacomini, P. Forck, D. Liakin, J. Dietrich, G. v. Villiers, "Ionization Profile Monitors at GSI", DIPAC'11, Hamburg, 2011, TUPD51.
- [7] T. Poikela et al., *Timepix3: a 65K channel hybrid pixel readout chip with simultaneous ToA/ToT and sparse readout*, Journal of Instrumentation, Volume 9, May 2014.
- [8] L. Giudicotti *Time dependent model of gain saturation in microchannel plates and channel electron multipliers*, Nucl. Instrum. Meth. A 659, 336 (2011).
- [9] A. Baumbaugh et al., *QIE10: a new front-end custom integrated circuit for high-rate experiments*, Journal of Instrumentation, Volume 9, January 2014.
- [10] R. Plackett et al., *Measurement of Radiation Damage to 130nm Hybrid Pixel Detector Readout Chips*, Topical Workshop on Electronics for Particle Physics, Paris, Sep 2009, pp.157-160.
- [11] S. Gilardoni, D. Manglunki et al., *Fifty years of the CERN Proton Synchrotron*, CERN-2011-004.
- [12] *LIU Proton Beam Parameters*, CERN-EDMS-1296306, September 2013.
- [13] *LIU PS Technical Design Report*, in preparation.
- [14] M. Sapinski, B. Dehning, A. Guerrero, M. Meyer, T. Kroyer, *Carbon Fiber Damage in Particle Beam*, HB'10, Morschach, 2010, MOPD61.
- [15] F.F. Rieke, W. Prepejchal, *Ionization cross sections of gaseous atoms and molecules for high-energy electrons and positrons*, Phys. Rev. A. 1972;6(4):1507.
- [16] F. Roncarolo, *Accuracy of the Transverse Emittance Measurements of the CERN Large Hadron Collider*, CERN-THESIS-2005-082.
- [17] E. Frojdh et al., *Count rate linearity and spectral response of the Medipix3RX chip coupled to a 300 μm silicon sensor under high flux conditions*, 15th international workshop on radiation imaging detectors, Paris, June 2013.
- [18] J.M. Belleman, *A New Trajectory Measurement System for the CERN Proton Synchrotron*, proceedings of DIPAC2005.
- [19] M. Patecki, *Analysis of LHC Beam Gas Ionization monitor data and simulation of the electron transport in the detector*, CERN-THESIS-2013-15.
- [20] D. Vilsmeier, B. Dehning, M. Sapinski, "Investigation of the Effect of Beam Space Charge on Electron Trajectories in Ionization Profile Monitors", MOPAB42, *These proceedings*, HB2014, East Lansing, USA (2014).
- [21] MAFalda website, developed by John Idarraga: <http://twiki.cern.ch/twiki/bin/view/Main/MAFalda>